Proceedings of the 8th International Conference on Civil Structural and Transportation Engineering (ICCSTE'23)
Canada – June 04-06, 2023
Paper No. 179
DOI: 10.11159/iccste23.179

Temperature Effects on Concrete Slab on Steel Girder Bridges with Malfunctioning Expansion Joints

Istemi F. Ozkan[1] and Husham Almansour[1]
[1]National Research Council Canada
1200 Montreal Road, Ottawa, Ontario, Canada K1A 0R6
istemi.ozkan@nrc-cnrc.gc.ca; husham.almansour@nrc-cnrc.gc.ca

Abstract – For both the design of new bridges and the evaluation of existing bridges, the quantification of the effects of thermal loads on structural behaviour is an important factor that needs to be taken into account. With the projected increase in average temperatures in Canada due to climate change, combined with deterioration, the demand on bridge infrastructure is expected to increase. Among the various deterioration issues in bridges, one of the most common is the malfunctioning of expansion joints. Due to the accumulation of debris and dirt in the joint, the axial movement of the bridge superstructure may be restrained, leading to axial forces at levels that the structural members are not originally designed for. It was also reported in the literature that the increasing temperature due to climate change may accelerate the overall deterioration rates and that of the expansion joints. This paper outlines a preliminary study on impacts of malfunctioning expansion joints on the structural behaviour and moment resistance of concrete slabs on steel girder (CSSG) bridges. A summary of temperature loads per the Canadian Highway Bridge Design Code (CHBDC) for various Canadian cities with different climates is first presented. A Finite Element Analysis (FEA) of a three-span continuous CSSG bridges is introduced and the results for axial load levels on this bridge with malfunctioning expansion joints are presented assuming that the bridge is situated at the location with the largest temperature loads among the locations considered. A brief literature review on the quantification of the moment resistance of CSSG bridges subject to interactions of axial force and shear is provided. Based on the FEA and literature review presented, future research considerations are proposed for temperature distribution and moment-shear-axial load interaction relationships on multi-span continuous CSSG bridges.

***Keywords*:** Steel, girder, axial load, deterioration, expansion joint

1. Introduction

For both the design of new bridges and the evaluation of existing bridges, the quantification of the effects of thermal loads on the bridge structural behaviour is an important factor that needs to be taken into account. Thermal effects on bridges can impact the design of the superstructure (especially the steel components), support bearings, and even the bridge piers [1]. With the projected increase in average temperature in Canada due to climate change [2], combined with deterioration, the demand on bridge infrastructure is expected to worsen [3].

Among the various deterioration issues in bridges, one of the most common is the malfunctioning of expansion joints [3]. Due to the accumulation of debris and dirt in the joints, the axial movement of the bridge superstructure may be restrained, leading to axial forces on the superstructure at levels that the structural members are not designed for. This paper outlines a preliminary study on the impacts of malfunctioning expansion joints on the structural behaviour and moment resistance of concrete slab on steel girder (CSSG) bridges. In section 2, a summary of temperature loads per the Canadian Highway Bridge Design Code (CHBDC) (2014) [4] for various Canadian cities with different climates is presented. In Section 3, the potential impacts of malfunctioning joints on bridge superstructure are further discussed including a brief literature review on the reduction in moment resistance of CSSG bridges subject to interactions of axial force and shear. In Section 4, a Finite Element Model (FEM) of a three-span continuous CSSG bridge is introduced, and in Section 5, the analysis results for axial load levels on a bridge with malfunctioning expansion joints are presented.

2. Temperature Effects

Reference [5] reports that the climate data in CHBDC 2014 and 2019 [4, 6] for temperature effects are based on historical data that assume climate stationarity, which is no longer valid as historical climatic data is no longer a reliable predictor of future climatic conditions and associated loads. It is understood that the 2025 iteration of the

CHBDC will include new climate change provisions that account for climate non-stationarity and are expected to lead to more climate-resilient bridges across Canada.

In order to demonstrate the thermal load levels for different climates of Canada, five major cities from east to west; namely, Halifax, Nova Scotia (NS); Montreal, Quebec (QC); Winnipeg, Manitoba (MB); Calgary, Alberta (AB); and Vancouver, British Columbia (BC) are selected. It should be noted that at the time of execution of this study, the CHBDC 2019 was not officially issued; thus, the temperature effects considered at the mentioned cities are based on CHBDC 2014 [4]. Columns (2) and (3) of Table 1 outline the minimum and maximum mean daily temperatures extracted from Figure A3.1.1–Maximum mean daily temperature and Figure A3.1.2–Minimum mean daily temperature of the CHBDC 2014 [4]. In order to take the effects of solar radiation and wind, the code requires modifications to be applied to the minimum and maximum mean daily temperatures extracted from Figures A3.1.1 and A3.1.2, respectively. Accordingly, the code requires the maximum mean daily temperatures (Column 3 of Table 1) to be increased by 20 ˚C and the minimum daily temperature (Column 2 of Table 1) decreased by 5 ˚C for steel girder bridges with concrete decks. CHBDC 2014 [4] requires that the temperature range obtained by the adjustments in Clause 3.9.4.1 to be further modified in accordance with the depth of the superstructure. As the depth of the bridge considered in Section 4 of this paper is over 2 m, the modifications to the effective temperatures are a 7˚C reduction for the maximum effective temperature and a 10˚C increase in the minimum effective temperature. The modified effective temperatures are presented in columns (4) and (5) of Table 1. Figure 1 illustrates the temperature ranges for the cities considered (Columns 4 and 5 in Table 1) as blue bars and the assumed construction temperature indicated by the orange line. Clause 3.9.4.2 recommends an effective construction temperature of 15°C in the absence of site-specific data. As directed by the code, when this temperature is used to determine the effective temperature ranges for the calculation of contraction and expansion, temperature changes outlined in Columns (6) and (7) are obtained. These are the values used as temperature loads in the analysis outlined in Section 4.

Table 1: Temperature effects per CHBDC 2014 [4].

City (1)	**Mean Daily Temperatures (˚C) per Figures A3.1.1 and A3.1.2**		**Effective Temperatures (˚C) per Table 3.8 of Clause 3.9.4.1**		**Modified Effective Temperatures (˚C) per Figure 3.5 of Clause 3.9.4.1**		**Temperature load assuming a 15 ˚C Construction Temperature**	
	Min. (2)	**Max. (3)**	**Min. (4)**	**Max. (5)**	**Min. (4)**	**Max. (5)**	**Contraction (6)**	**Expansion (7)**
Halifax (NS)	-22	26	-27	46	-17	39	-32	24
Montreal (QC)	-34	30	-39	50	-29	43	-44	28
Winnipeg (MB)	-37	31	-42	51	-32	44	-47	29
Calgary (AB)	-38	27	-43	47	-33	40	-48	25
Vancouver (BC)	-14	28	-19	48	-9	41	-24	26

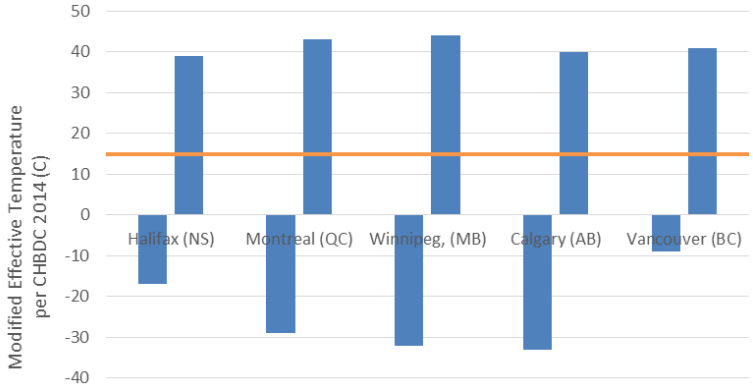

Fig. 1: Modified Effective Temperature per CHBDC (2014) [4] for a CSSG bridge with a superstructure depth over 2m.

The code also requires the effects of thermal gradients through the depth to be considered in the design per Clause 3.9.4.4. In this preliminary study, for practical reasons, temperature load values in columns (6) and (7) of Table 1 are applied uniformly to the bridge analyzed in Section 4.

It should be noted that the temperature modifications prescribed in Clause 3.9.4.1 and gradient in Clause 3.9.4.4 prescribed by the code are based on studies from the 1970s and early 1980s [7, 8, 9] on deep concrete bridges with the assumption that they apply to CSSG bridges as well. It is not clear how these may be applicable in the current and projected climates. Various, relatively newer, studies are available in the literature that propose temperature distribution/gradient over the bridges (e.g., [1, 10, 11, 12]) which also question the accuracy of temperature gradient models in applicable codes (i.e., AASHTO). Further studies on the estimation of temperature distribution on CSSG bridges accounting for the impacts of climate change may be needed.

3. Deterioration of Expansion Joints

According to Palu and Mahmoud [3], among the various deterioration issues that impact bridges, one of the most common is the malfunctioning of expansion joints. In their study, they also reported that the most vulnerable bridges to potential structural issues due to expansion joint deterioration coupled with climate change-induced elevation in temperatures are the ones in the regions of the U.S. bordering Canada (i.e., Northern Rockies & Plains, Northwest and Upper Midwest). Therefore, similar issues may be expected for Canadian bridges. Increases in the frequency of days with persistent air temperatures exceeding 32°C can induce pavement softening and traffic-related rutting, as well as degradation in highway and bridge expansion joints, according to [13]; therefore, with increasing temperatures due to climate change, deterioration of expansion joints may accelerate.

Bridge girders are designed for bending and shear; however, under the condition of malfunctioning joints, the girders would be subjected to bending and shear due to dead and traffic load simultaneously with thermal axial load due to expansion restriction [3]. Potential levels of axial force on bridges with malfunctioning expansion joints are demonstrated in Section 4. Interaction relationships that allow for the prediction of the remaining moment capacity of a composite CSSG bridge segment subject to shear and axial forces are available in the literature and are further discussed in Section 5; however, the applicability of these relationships to Canadian CSSG bridges is not apparent and require further evaluation.

4. Analysis of a CSSG Bridge

4.1. Description of the Bridge

A straight 3-span continuous bridge is considered with 60 m spans. Figure 2a illustrates the cross-section of the bridge analysed. Bridge deck is selected as 17,120 mm wide. The overall bridge width is 18,000 mm laying over five fabricated I-girders. The concrete deck is 250 mm deep including a 15 mm wearing surface. The girders are equally spaced at 3,600 mm centre-to-centre. Distance between the centreline of the outer girders and the outside of the deck is 1,800 mm on both sides. The beam web depth is selected as 2,100 mm with a thickness of 25 mm throughout the bridge. Flange thicknesses and widths vary along the bridge for the span girders and the support girders. The distribution of the girder sections along the bridge are shown in Figure 2b. For the analysis of the pristine expansion joints, from left to right, support 1 (i.e., left abutment), support 3, and support 4 (i.e., right abutment) were considered as roller supports allowing longitudinal movement. Support 2 was considered as a pin support that restrains longitudinal movement. For the analysis of the malfunctioning expansion joint case, the roller supports on the abutments were switched to pin supports that do not allow for longitudinal movement.

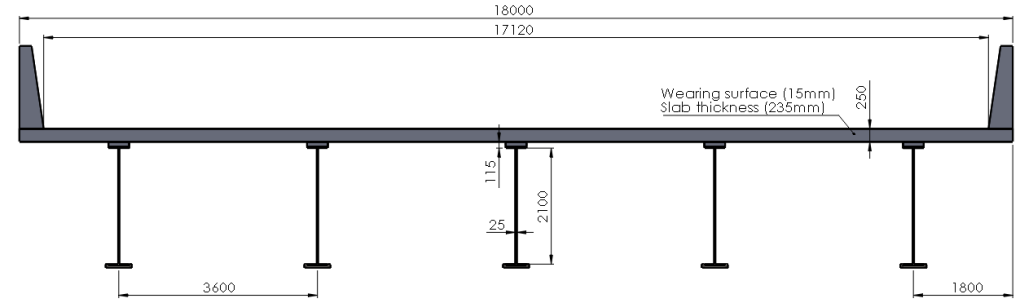

(a) Cross-section view of the bridge

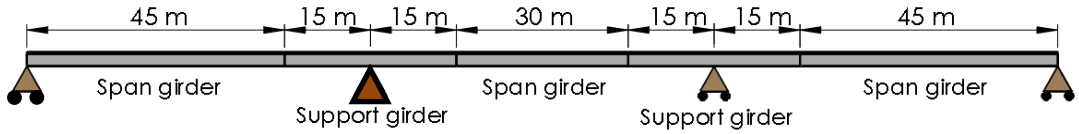

(b) Side view of the bridge – pristine support conditions

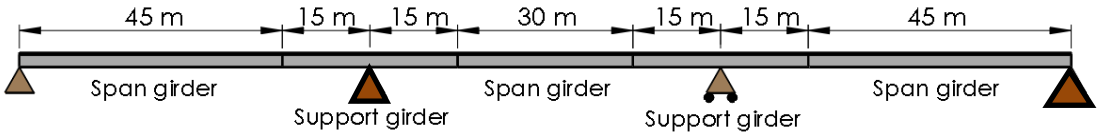

(c) Side view of the bridge – clogged abutment supports

Fig. 2: Concrete Slab on I-girder Bridge Analyzed.

4.2. Sectional Axial Load Capacity

The effective slab width that would contribute to the composite action of concrete deck and steel girder is calculated to be 3600 mm with a structural depth of 235 mm excluding the 15 mm wearing surface for both span and support girders. Figure 3 presents these segments. Table 2 presents the axial load capacity of the composite sections shown in Figure 3. The axial load capacity is calculated based on the cracking strain of concrete under compression. The contribution of steel reinforcement is ignored.

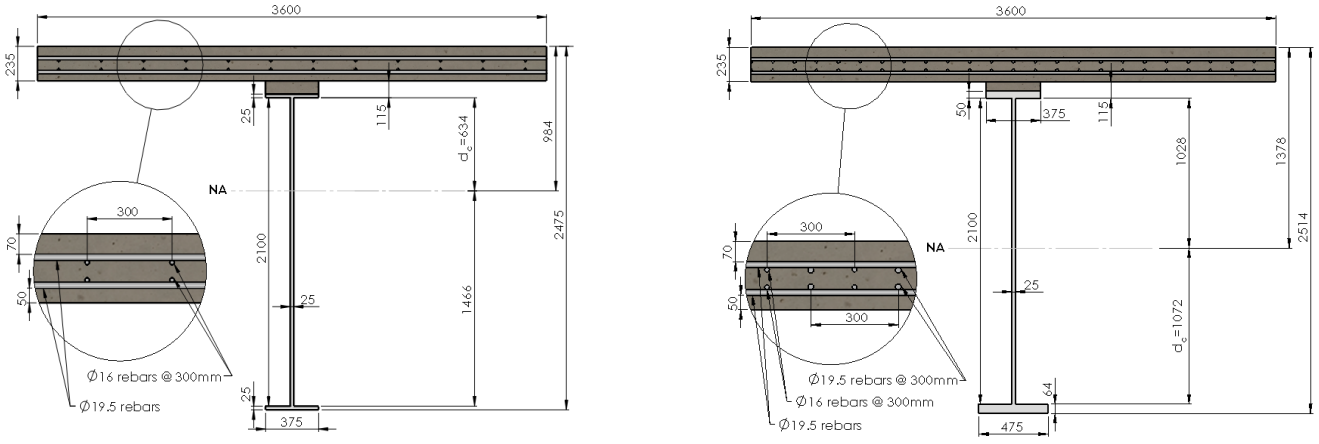

(a) Span segment composite load carrying unit (b) Support segment composite load carrying unit

Fig. 3: Composite load carrying segments.

Table 2: Axial load capacity for the composite sections in Figure 3
(ignoring the reinforcing bars and assuming that the steel girder and the concrete slab are fully bonded).

	Span segment girder (see Figure 3a)	Support segment girder (see Figure 3b)
Steel girder cross-section area (mm^2)	71,250	101,650
Steel yield strength (MPa)	350	350
Axial capacity of the steel girders (kN)	24,938	35,578
Concrete slab area (mm^2)	846,000	846,000
Concrete compressive strength (MPa)	30	30
Concrete slab compressive capacity (kN)	25,380	25,380
Steel girder load level when concrete crushes assuming that steel and concrete are fully bonded (kN)	17,238	24,593
Axial load capacity for the composite section (kN)	42,618	49,973

4.2. Description of the FEA Model

CSi Bridge software is used for the analysis of the bridge considered. Both girders and deck were modelled using shell elements. The default meshing of the software was utilized. A sensitivity analysis for the element size/numbers was not deemed necessary for this preliminary study. All the analyses conducted were linear elastic. Two materials were defined to represent the concrete and steel members of the bridge. The elastic properties of these materials used as inputs of the model are outlined in Table 3.

Table 3: Material properties.

	Concrete slab material	Steel girder material
Weight per unit volume (N/mm^3)	2.356E-05	7.697E-05
Modulus of elasticity (MPa)	24,800	200,000
Poisson's ratio	0.2	0.3
Coefficient of thermal expansion	9.90E-06	1.170E-05
Concrete compressive strength (MPa)	30	N/A
Steel yield strength (MPa)	N/A	350

For the representation of the dead loads on the bridge, three dead load components were user-defined for self-weights of girders, barriers, and deck. Girder self-weight was modelled as linearly distributed load applied to the deck over the centre-line of the girders as 6.27 N/mm. No distinction in self-weight was made between the girder segments. The uniform linear girder load was calculated by dividing the total girder weight by the total length of the girders (180 m). Barrier loads are also defined as linearly distributed loads applied 220 mm inside from both edges of the deck. Deck weight and the wearing surface weight were modelled as distributed area loads and spread over the deck of the bridge uniformly. As for live loads, CL-625 Truck load and CL-625 Lane load were selected per CHBDC 2014 [4] and the analysis was conducted to output the most detrimental axial load envelope for five design lanes, where the number of design lanes were according to Table 3.5 of CHBDC [4].

4.3. FEA Outputs

4.3.1 Axial Force Envelope – Pristine Expansion Joints

Figure 4 illustrates the envelope for the axial force ratio, A_n, (axial force predicted by the FEA model-to-Axial load capacity for the composite section from Table 2). The analysis is based on following parameters/assumptions; (1) the

bridge is assumed to be located in the City of Winnipeg since the largest expansion is expected at this location based on the temperature analysis outlined in Table 1; (2) the analysis is based on CHBDC Ultimate Limit State (ULS) 2 load combinations; and (3) the boundary conditions are according to Figure 2b (i.e., free axial deformation at ends A and B; no expansion joint restraints due to malfunctioning). Behaviour due to cooling temperature change is not included in the plot since the expansion joint malfunctioning is assumed not to affect contracting. As expected, the axial force levels on the composite section are negligible when compared to the cross-sectional axial force capacities of 42,618 kN and 49,973 kN for the span and support segments (below 2%), respectively.

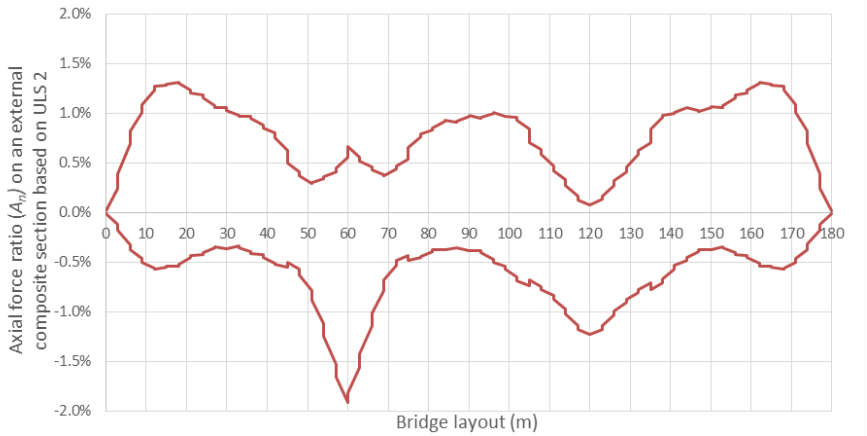

Fig. 4: Axial force ratio (A_n) based on ULS 2 for the original pristine expansion joint case (assumption: the bridge is location in the City of Winnipeg).

4.3.2 Axial Force Envelope – Malfunctioning Expansion Joints

Figure 5 illustrates the axial force ratio (A_n) envelope for one of the external composite sections based on the boundary conditions in Figure 2c (i.e., restrained axial deformation at ends A and B; expansion joints are malfunctioning). The plot only demonstrates the axial compressive force levels that may potentially arise due to warming. The axial load levels may reach over 30% of the cross-sectional capacity for the specifics of the bridge selected. For a continuous span bridge, the interaction of the axial forces with shear may impact the moment capacity of a bridge both in span and support segments. In such circumstances, interaction relationships may be needed for the prediction of the moment capacity.

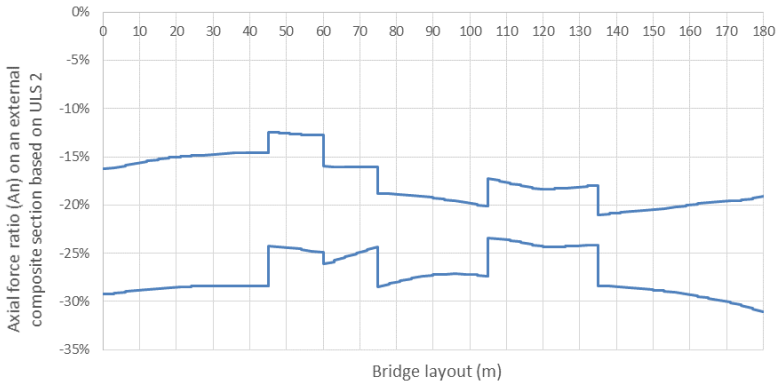

Fig. 5: Axial force ratio (A_n) based on ULS 2 for the malfunctioning expansion joint

5. Moment – Shear – Axial Interaction

A series of studies from the University of Western Sydney, Australia, report a set of non-dimensional interaction diagrams for combinations of moment (positive/negative) – shear – axial force (compression/tension) on composite CSSG bridges as noted in [14, 15, 16, 17, 18]. For instance, negative bending – axial compression interaction diagram proposed

by Vasdravellis et al. [14] is a linear relationship and it is found that approximately 25% axial compression at the supports of the analyzed bridge in Section 4 may lead to a 25% reduction of its negative moment capacity if the shear at these locations is ignored. When shear is considered, this reduction in moment capacity is expected to be larger.

These interaction diagrams are based on reduced-scale laboratory tests on composite CSSG segments and exhaustive parametric numerical experimentation with relatively large slab-to-beam aspect ratios and compact steel sections. The authors recognize that more tests and numerical analyses should be conducted to expand the interaction diagrams to composite girders having different slab-to-beam aspect ratios and slenderness [18], which are commonly used in Canadian bridges.

6. Conclusive Remarks and Future Research

The level of axial compression on a bridge depends on a number of factors including temperature change (warming) levels, environmental factors such as exposure to sunlight and wind, the length of the segments between expansion joints, how the expansion joints may behave when malfunctioning (i.e., boundary conditions), etc. Whether climate change effects are included or not, potentially malfunctioning joints (i.e., restraining expansion due to clogging) may lead to significant axial load levels on bridge girders. For instance, the axial compression level on the bridge analysed in this study was observed to exceed 30% of its axial load capacity when its expansion joints were restrained in their movement. Based on the findings of this study, further research is proposed in the following two areas:

(1) Thermal gradient on deep CSSG bridges:
CHBDC requires the effects of thermal gradients through the depth to be considered in the design of composite CSSG bridges. However, the thermal gradient model prescribed by the code is based on studies from the 1970s and early 1980s on deep concrete bridges and their applicability to deep steel girder bridges in a changing climate is not apparent. Various, relatively newer, studies are available in the literature that propose temperature distribution/gradient over CSSG bridges. The applicability of these new thermal gradient models to Canadian bridges needs to be further studied.

(2) Applicability of moment-shear-axial force interaction diagrams to Canadian bridges:
A set of non-dimensional interaction diagrams for combinations of moment (positive/negative) – shear – axial force (compression/tension) on composite CSSG bridges are available in the literature. However, the applicability of these interaction diagrams to Canadian bridge designs is not clear. A numerical parametric study is proposed to evaluate the applicability of these interaction diagrams to Canadian bridges, especially those with deep steel girders.

Acknowledgements

The study presented in this paper is conducted by funding from Infrastructure Canada through the Climate Resilient Buildings and Core Public Infrastructure (CRBCPI) and Climate Resilient Built Environment (CRBE) initiatives of the National Research Council Canada.

References

[1] C. Quan, “Effects of thermal loads on Texas steel bridge,” *University of Texas Library,* 1 08 2008.

[2] S. Cohen, E. Bush, X. Zhang, N. Gillett, B. Bonsal, C. Derksen, G. Flato, B. Greenan and E. Watson, “Canada's Changing Climate Report,” Government of Canada, Ottawa, 2019.

[3] S. Palu and H. Mahmoud, “Impact of climate change on the integrity of the superstructure of deteriorated U.S. bridges,” *PLOS ONE,* vol. 14, no. 10, 2019.

[4] C. Group, Canadian Highway Bridge Design Code, Toronto: CSA Group, 2014.

[5] D. Kennedy, H.-P. Hong, J. Fyke and D. Gagnon, “Climate Change Provisions for CSA S6:25 Canadian Highway

Bridge Design Code: Findings and Recommendations," CSA Group, Toronto, 2022.

[6] C. Group, Canadian Highway Bridge Design Code, Toronto: CSA Group, 2014.

[7] R. Green and M. Radolli, "Thermal Stresses in Concrete Super Structures Under Summer Conditions," *Transportation Research Record,* no. 547, 1975.

[8] M. M. Elbadry and A. Ghali, "Temperature Variations in Concrete Bridges," *ASCE Journal of Structural Engieering,* vol. 109, no. 10, pp. 2355-2374, 1983.

[9] J. H. Emanuel and J. L. Hulsey, "Temperature Distributions in Composite Bridges," *ASCE Journal of the Structural Division,* vol. 104, no. 1, pp. 65-78, 1978.

[10] D. Wang, B. Tan, X. Wang and Z. Zhang, "Experimental study and numerical simulation of temperature gradient effect for steel-concrete composite bridge deckExperimental study and numerical simulation of temperature gradient effect for steel-concrete composite bridge deck," *Measurement and Control,* vol. 54, no. 5-6, 2021.

[11] R. Hagedorn, "Impact of Extreme Summer Temperatures on Bridge Structures," *ScholarWorks@UARK,* 2016.

[12] G. D. Zhou and T. H. Yi, "Thermal Load in Large-Scale Bridges: A State-of-the-Art Review," *International Journal of Distributed Sensor Networks,* vol. 2013, 2013.

[13] H. G. Schwartz, M. Meyer, C. J. Burbank, M. Kuby, C. Oster, J. Posey, E. J. Russo and A. Rypinski, "Climate Change Impacts in the United States: The Third National Climate Assessment," U.S. Global Change Research Program , 2014.

[14] G. Vasdravellis, B. Uy, E. L. Tan and B. Kirkland, "Behaviour and design of composite beams subjected to negative bending and compression," *Journal of Constructional Steel Research,* vol. 79, 2012.

[15] G. Vasdravellis, B. Uy, E. L. Tan and B. Kirkland, "The effects of axial tension on the sagging-moment regions of composite beams," *Journal of Constructional Steel Research,* vol. 72, 2012.

[16] G. Vasdravellis and B. Uy, "Shear Strength and Moment-Shear Interaction in Steel-Concrete Composite Beams," *Journal of Structural Engineering,* vol. 140, no. 11, 2014.

[17] G. Vasdravellis, B. Uy, E. L. Tan and B. Kirkland, "Behaviour and design of composite beams subjected to sagging bending and axial compression," *Journal of Constructional Steel Research,* vol. 110, 2015.

[18] B. Kirkland, P. Kim, B. Uy and G. Vasdravellis, "Moment–shear–axial force interaction in composite beams," *Journal of Constructional Steel Research,* vol. 114, 2015.